Title
The prediction of indoor air motion for occupant cooling in naturally ventilated buildings

Authors
Ernest, D.
Bauman, Fred
Arens, Edward A

Publication Date
1991

Peer reviewed

NY-91-5-5

THE PREDICTION OF INDOOR AIR MOTION FOR OCCUPANT COOLING IN NATURALLY VENTILATED BUILDINGS

D.R. Ernest

F.S. Bauman, P.E.
Member ASHRAE

E.A. Arens, Ph.D.
Member ASHRAE

ABSTRACT

This paper describes the development of an empirical model for the prediction of wind-induced indoor air motion in naturally ventilated buildings, as needed for the assessment of thermal comfort. The model is based on correlations developed from a large set of experimental pressure and velocity data collected from architectural models in a boundary layer wind tunnel. The goal of the study was to examine and formalize the relation between indoor air motion parameters (velocities and turbulence intensities) and the external surface pressure distribution on sealed models for which data bases and correlations are now available. This was accomplished through two series of tests. In the first, indoor air speed and turbulence intensity distributions were measured in models with openings for various wind directions and building configurations. In the second, the external surface pressure distribution was measured on a sealed model for the same building configurations. The number of architectural configurations tested, which were selected to cover a wide range of possible building-airflow interactions, included the effects of wind direction, upwind obstructions, building shape, window size, and other architectural features such as wing walls and roof overhangs. The resulting correlations, based on nearly 300 tests, predict indoor air motion with a good level of accuracy as a function of wind direction, window size, and the external pressure distribution measured on sealed models.

INTRODUCTION

Natural ventilation can be used as an energy-conserving design strategy to reduce building cooling loads and improve indoor thermal comfort in many hot-climate areas. Moreover, in many developing countries where air-conditioning systems do not represent a realistic alternative, natural ventilation may be the only cooling strategy available.

The cooling effects of wind-driven natural ventilation inside buildings are governed by three fundamental mechanisms:

1. Under proper conditions, wind-driven airflows can offset internal and solar heat gains by replacing warm indoor air with cooler outside air, thus lowering indoor air temperature.
2. Natural airflow through the building can cool down its structure, carrying away the sensible heat stored in its thermal mass. This results in lower radiant temperatures in the space. This principle is applied in precooling buildings at night in hot, dry climates.
3. Induced indoor air motion can also cool building occupants directly by increasing convective and evaporative heat loss from the occupant's body surfaces.

In the recent past, numerous studies have focused on the first mechanism, and models using surface pressure coefficients are now being developed to predict airflow rates in buildings (Bauman et al. 1988; Swami and Chandra 1988). The second mechanism is also receiving attention. ASHRAE recently sponsored a detailed laboratory study of room convective heat transfer for interior walls subjected to high ventilation rates, with the aim of producing a predictive method to be incorporated into computerized building energy simulation programs (Pedersen et al. 1990). Very little work, however, has been undertaken on the third mechanism. This aspect of natural ventilation (dealing with occupant cooling) has been difficult to assess, since it requires the prediction of indoor air movement.

The effects of indoor air motion on human thermal comfort in hot environments have been extensively studied, and it is now well established how air movement can offset increases in air temperature. Air velocities increase the body's convective and evaporative heat loss rate. Several researchers have studied the effect of air velocities on thermal comfort (McIntyre 1978; Arens et al. 1986; Jones et al. 1986; Chang et al. 1988; Scheatzle et al. 1989; Tanabe and Kimura 1989). Moreover, it has been shown recently that the impact of air turbulence intensity on comfort can also be significant (Mayer 1987; Fanger et al. 1988). It is expected that the effects of turbulence will soon be integrated into human thermal comfort models, probably in the form of an "effective velocity" as used in exterior wind comfort studies (Arens et al. 1989).

To predict the acceptability of a naturally ventilated indoor environment to its occupants, it is necessary to determine wind-driven interior velocity and turbulence intensity distributions. Furthermore, with the current move to incorporate comfort models in building energy simulation programs (to reflect the fact that HVAC strategies should be

David R. Ernest is a Ph.D. Candidate, **Fred S. Bauman** is a Research Specialist, and **Edward A. Arens** is a Professor in the Department of Architecture, University of California, Berkeley.

targeted for people rather than buildings), it becomes necessary to fully account for the effect of indoor air movement (for example, Coutier et al. [1985] recently added a comfort model to BLAST).

Nonconditioned air movement required for comfort in buildings can be induced by external winds, whole-house fans, or ceiling fans (indoor velocities induced by thermal stack effect are generally too low). Wind-driven natural ventilation is particularly appealing, since it uses no auxiliary power and only requires controllable openings in the building envelope. However, if the concept of natural ventilation is to be useful to designers and architects, methods and design tools are needed to predict its effectiveness. Such tools currently do not exist. This stems from there being no simple methods to predict wind-induced air velocity distributions inside buildings.

There are currently five different methods for estimating wind-induced indoor air motion: (1) full-scale measurements, (2) numerical simulations, (3) use of published tabulated data based on parametric wind tunnel studies, (4) use of the wind discharge coefficient method, and (5) direct measurement of the indoor velocities in scale models in a boundary layer wind tunnel.

Full-scale field studies of indoor air motion can only be used to evaluate existing buildings (Chand et al. 1989) and are essentially useful for the validation of the other predictive methods (Chandra et al. 1982; Gandemer and Barnaud 1989).

The numerical computer simulation of indoor air motion, which is still in a developmental stage, is both too complex and inappropriate for design applications of natural ventilation (Mathews 1989; Tsutsumi et al. 1988; Kurabuchi and Kusuda 1987; Holmes and Whittle 1987).

Published sources of tabulated interior velocity levels resulting from generalized wind tunnel tests on generic models are available. The effects of a number of building parameters on indoor air motion have thus been reported (Chand et al. 1968, 1969, 1970, 1975, 1978; Givoni 1962, 1965, 1969; Sobin 1981, 1983). Overall, while they provide important design guidelines, the results of these experiments cannot be used to actually predict indoor air movement for a representative range of building and flow configurations due to the following important limitations:

1. They do not adequately account for the effects of external building geometry and wind characteristics on interior flow properties. For example, the actual pressure differentials between inlet and outlet were not varied. In addition, the turbulent nature of the airflow around buildings was rarely modeled.

2. The blockage of the wind tunnel by the model during these tests was often excessive, influencing the reliability of results.

3. Upwind obstructions were rarely considered, although they represent the typical building configuration (Chand et al. 1975).

4. Only a limited number of simplified interior space configurations were tested.

5. Interior air turbulence intensities were not measured.

6. The measured interior velocities cannot be related to local climatic data.

External surface pressure coefficients (C_p) measured on sealed models can be used to estimate velocities at inlets or through narrow corridors (Aynsley 1982). The calculations make use of discharge coefficients (C_d) to account for the characteristics of the inlet and outlet geometries. However, only conservative estimates of velocity levels in the occupied space, away from inlet areas, can be derived from this method (Arens and Watanabe 1986).

Finally, the direct measurement of interior airflows in scale models placed in a boundary layer wind tunnel has been shown to be a useful, simple, and accurate technique for the prediction of indoor air motion (Aynsley 1982; Poreh et al. 1982; Cermak et al. 1982). A method using this technique has been developed to predict thermal comfort levels in a naturally ventilated building (Arens et al. 1984). Unfortunately, the use of such methods, requiring access to a wind tunnel, is impractical for most building designers, especially for small housing projects.

Objective of the Study

The purpose of this study was to develop a simple method for the prediction of indoor air motion in naturally ventilated buildings, as needed for the assessment of indoor thermal comfort. To be truly useful, this method must be such that it is readily accessible to the design community. In practical terms, this means that the method should be integrable in computerized procedures that operate on full sets of hourly climate data.

APPROACH

For the purpose of assessing the impact of complex, wind-induced indoor airflows on the overall thermal comfort conditions in a given space, one only needs

1. a measure of the overall interior air movement intensity in the occupied space, including the effects of both velocity and turbulence, and

2. a measure of the air movement spatial distribution within the interior.

Based on these two indoor air motion parameters, one can retrieve the approximate air movement distribution in the space and, combined with other thermal environment parameters, use it to assess comfort levels. Although more detailed local flow characteristics in the room can influence thermal comfort conditions, such a level of detail is beyond the scope of a practical prediction method.

In porous buildings exposed to relatively strong winds, indoor air motion will be greatly influenced by the external pressure distribution around the building. It is therefore convenient to relate it to building surface pressure coefficients (C_p), for which large data bases and correlations are now available (Swami and Chandra 1988; Balazs 1989). In this study, the relation between the indoor air motion parameters (velocities and turbulence levels) and the external pressure distribution on sealed models was examined and formalized.

This was accomplished through two series of tests conducted at model scale in a boundary layer wind tunnel. In the first, indoor air speed and turbulence intensity distributions were measured in models with openings for various wind directions and building configurations. In the second, the external surface pressure distribution was measured on sealed models for the same building configura-

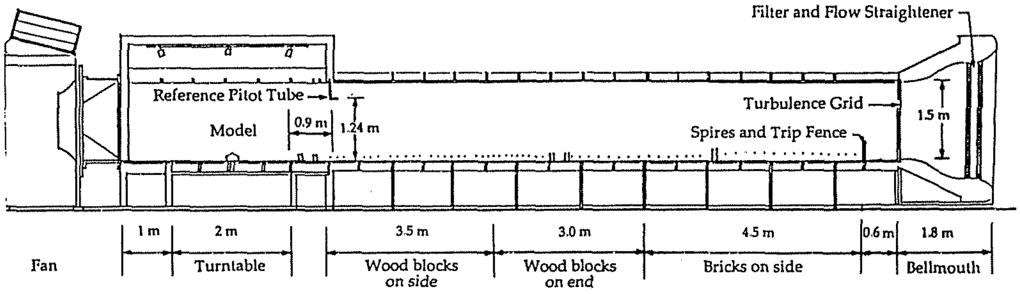

Figure 1 *Boundary layer wind tunnel*

tions. The two sets of data were then analyzed to produce correlations for predicting indoor air motion parameters as a function of wind direction, window size, and the external pressure distribution measured on the sealed models.

The implications of using data obtained from two physically different building models—one that is porous and the other sealed—are discussed briefly below. First, the overall external pressure field around the building may be affected by the presence of wall openings in the structure. This effect was investigated by Snyckers (1970), who found that the presence of fairly large openings of various shapes (wall porosity of 12%) did not significantly affect the surface pressure distribution patterns except in the immediate vicinity of the openings.

Second, as pointed out by Aynsley (1988), the effective driving force responsible for the airflow through the building is the difference between the total pressure at the inlet (including a velocity pressure component), and the static pressure at the outlet. Pressures measured on window areas of sealed models may be different from those measured at the open windows of porous models. For example, Poreh et al. (1982) found that the total pressure measured at an open inlet was slightly larger than the pressure measured on a sealed model at the same location. To account for this effect, estimates of the pressure distribution at open windows would therefore be required. These are difficult to measure directly, especially for oblique wind directions, and very little published data are currently available. However, studies that have addressed this issue have shown that the use of pressures measured on sealed models, rather than the actual pressures, lead to errors of less than 10% for predicted flow rates (Aynsley 1988).

Finally, in another study, it was found that for buildings with wall porosities lower than about 25% and wind angles below 45°, internal airflow rates could be predicted to within 10% from external surface pressure distributions measured on sealed models (Vickery and Karakatsanis 1987). These studies suggest that the use of pressure distributions on sealed models are appropriate for the prediction of indoor air motion in open models with low porosities.

In this study, the wind tunnel tests were performed to investigate wind-induced indoor air motion and flow patterns in relation to the following parameters: (1) upwind terrain roughness, (2) wind direction, (3) immediate upwind obstructions, (4) external building shape, and (5) window size. The effects of other parameters, such as interior room partitions and window location, are reported in Ernest et al. (1990).

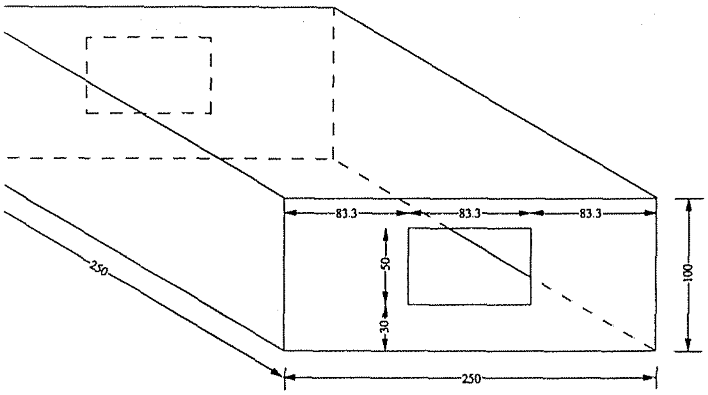

Figure 2 *Exterior model dimensions (mm)*

EXPERIMENTAL METHODS

Boundary Layer Wind Tunnel

In this study, both the indoor velocity and surface pressure experiments were conducted in an open-circuit boundary layer wind tunnel located in a university laboratory. As shown in Figure 1, the first 42 ft (12.8 m) of the wind tunnel correspond to the flow-processing section in which a combination of turbulence-generating devices and rough objects cover the floor to simulate the characteristics of the flow approaching the building model. Immediately downwind of the flow-processing section is a 12 ft (3.7 m) long test section, in which the scale models are placed on a 6.6 ft (2 m) diameter rotating turntable for testing. The pressure and velocity instrumentation is mounted below the turntable. A PC-based data acquisition system located in an adjacent chamber was used to collect and analyze the experimental data.

Building Models

For this study, two single-room models were fabricated out of 1/8-in. (3-mm) transparent acrylic sheet. Model 1, used for velocity measurements, had reconfigurable openings. Model 2, used for surface pressure measurements, was completely sealed and equipped with pressure taps. The overall dimensions of the models are 3.94 in. (100 mm) high, 9.84 in. (250 mm) long, and 9.84 in. (250 mm) wide (see Figure 2 for Model 1 with the base case openings). This corresponds to a scale of 1:30 based on the interior space dimensions. The size of the models was selected to be large enough to maximize the internal Reynolds number (Re_i) but small enough to limit the maximum wind tunnel blockage and allow adequate modeling of the boundary layer. These instrumented models were used in conjunction

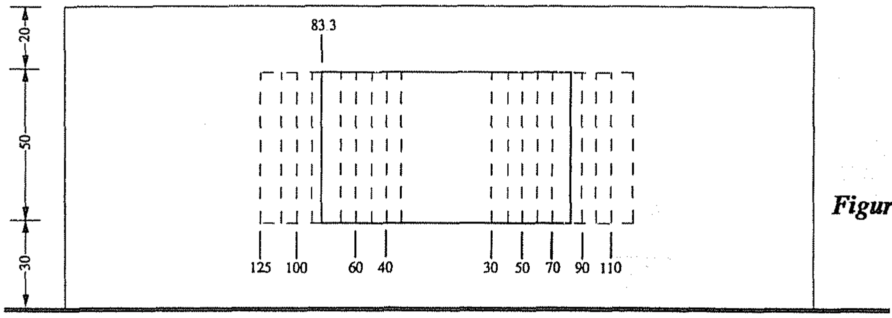

Figure 3a *Window configurations (Model 1)*

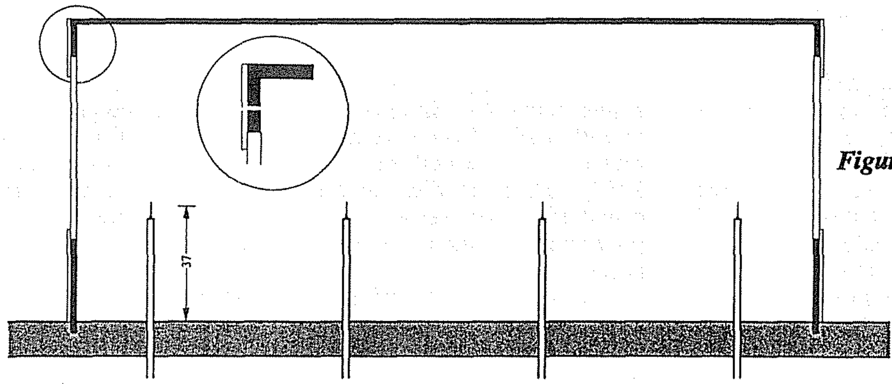

Figure 3b *Cross section of Model 1 showi sensor locations*

with uninstrumented polystyrene blocks to assemble the various building geometries tested.

The two opposite façades of Model 1 have a large open area (8.66 in. by 2.36 in. [220 mm by 60 mm]) on which window frames of various sizes can be fitted. Figure 3a shows the various window sizes investigated on Model 1, with a solid line representing the base case window. The height of the window was kept constant at 1.97 in. (50 mm), with the sill at 1.18 in. (30 mm) and the lintel at 3.15 in. (80 mm). The window width, on the other hand, could be varied from 1.97 in. (30 mm) to 4.92 in. (125 mm). The corresponding wall porosities, defined as the ratio of the window area to the area of the wall containing it, varied from 6% to 25%. The base case window width was 3.28 in. (83.3 mm), corresponding to one-third of the wall width and a porosity of 16.7%. The thickness of the window frames is fairly thin (less than 0.039 in. [1 mm]), allowing a clear separation of the flow to occur at the window edge (see Figure 3b).

A row of four velocity sensors was installed on the centerline of the turntable through holes in the wind tunnel floor. The model was placed directly above the sensors, so that the row of probes was parallel to the model inlet-outlet axis (Figure 3b). Spacing between probes (2.40 in. [61 mm]) was based on an equal-area coverage for each probe. The height of the sensors inside the model was selected to be representative of the occupied level in the room. It was

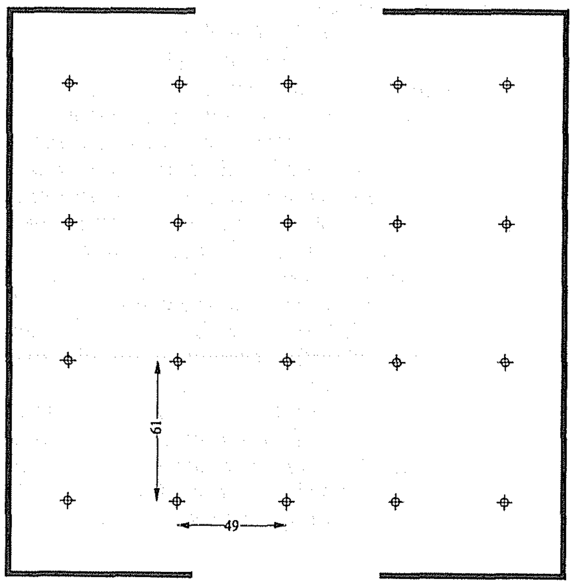

Figure 3c *Velocity measurement locations (Model 1)*

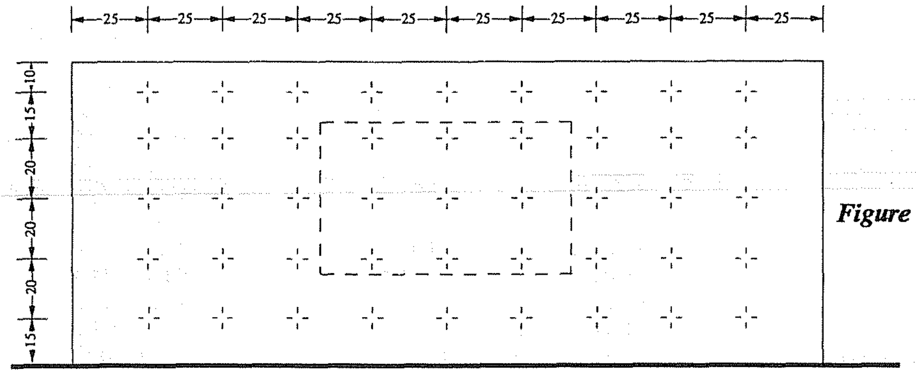

Figure 3d *Pressure tap locations (Model 2)*

fixed at 1.46 in. (37 mm), the equivalent of 3.6 ft (1.1 m) full-scale, corresponding to head height for a seated person and mid-body height for standing subjects. Rather than moving the row of probes inside the model, tracks on the floor allowed the model to be moved laterally as required for indoor velocity measurements at five different row locations, corresponding to a total of 20 measurement points per configuration (see Figure 3c). The spacing between each row location was 1.93 in. (49 mm), corresponding to one-fifth of the interior width of Model 1.

For Model 2, the pressure tap distribution was selected so that surface pressures could be measured over areas corresponding to openings on Model 1. The two opposite faces of the model were equipped with 45 pressure taps each (Figure 3d); 9 pressure taps symmetrically covered the base case window area. The maximum wind tunnel blockage occurs when the instrumented model (or base case model) is used in conjunction with other building blocks and is less than 2.5%. No corrections due to blockage effects were made on measurements obtained with these model configurations.

Mean Velocity and Turbulence Intensity Measurements

Four anemometers were used in conjunction with custom-built, high-frequency response, vertical hot-film probes for the measurement of indoor air motion. These sensors have the advantage of being able to measure the horizontal velocity fields (as experienced by human subjects) for high-frequency turbulence intensity airflows.

Preliminary tests showed that the self-shielding effect of the probes on other probes located further downstream in the row parallel to the flow had a negligible impact on indoor velocity and turbulence measurements due to the highly fluctuating nature of the interior flows. It was also found that the lateral movement of the model (±3.86 in. [±98 mm]) did not affect the measurement results due to the largely two-dimensional nature of the flow in the center of the test section of the tunnel and the small longitudinal variation of the mean velocity at the model location.

For velocity and turbulence intensity measurements, the output voltage of each anemometer was sampled at a frequency of 30 Hz for a period of 30 seconds. When needed, a temperature correction was applied to this voltage.

For each building configuration tested, and based on the 20 measurements per test, three nondimensional indoor air motion parameters were computed:

$$C_v = 1/n \sum_{i=1}^{n} (V_i/V_e) \tag{1}$$

$$C_{sv} = \sigma_s(V_i)/(V_e \cdot C_v) \tag{2}$$

$$C_t = 1/n \sum_{i=1}^{n} \sigma_t(V_i)/(V_e \cdot C_v) \tag{3}$$

where

C_v = average velocity coefficient
C_{sv} = coefficient of spatial variation
C_t = average turbulence coefficient
V_i = mean velocity at interior location i (m/s)
V_e = mean outdoor reference freestream velocity at eave height (m/s)
$\sigma_s(V_i)$ = standard deviation of the n mean interior velocities (m/s)
$\sigma_t(V_i)$ = standard deviation of the fluctuating component of V_i (m/s)
n = number of interior measurement locations in the model (20).

C_v is the measure of the relative strength of the interior air movement in the horizontal plane representative of the occupied space of the room. C_{sv} is a nondimensional measure of the relative spatial uniformity of that flow. A low C_{sv} indicates a rather uniform flow, and a high value represents a greater spatial unevenness for the interior velocity distribution. Finally, C_t is an overall measure of the turbulence level in the room.

For simplicity, the convention selected was to reference the velocity coefficients, C_v, to the freestream velocity at the building's eave height (3.94 in. [100 mm] or 9.84 ft [3 m] full scale). This allows the indoor velocity to be expressed as a percentage of the available outdoor wind. A simple correction factor can then be applied to the velocity coefficient to relate it to local full-scale climatic data.

In this study, however, the outdoor reference velocity was measured at the beginning of each test at the standard probe height of 1.46 in. (37 mm) with the model removed. A correction factor was then applied to this measured reference velocity to account for the height effect. This height-correction factor, the ratio of the velocity at eave height (3.94 in. [100 mm]) to the velocity at 1.46 in. (37 mm) in the approach flow, was determined in a separate independent test. The maximum error associated with the mean velocity measurements is estimated to be 15%.

Pressure Measurements

Two differential pressure transducers were used in the experimental setup: transducer #1 measured the mean surface pressure of each individual tap on the model and transducer #2 monitored the freestream dynamic and static pressures at the reference pitot tube in the wind tunnel (see Figure 1).

Each pressure tap on the model was connected via a 2.0 ft (0.6 m) long, 0.063 in. (1.6 mm) O.D. vinyl tube to a rotary valve that allowed each tap to be sequentially connected to a single pressure transducer. The pressure at each tap of the building model was measured simultaneously with the reference dynamic pressure at the pitot tube. The transducers were sampled at a rate of 10 Hz for a duration of 15 seconds. Upon switching to a new port position on the pressure switch, a delay of 10 seconds was implemented to allow the pressure line to stabilize to its new value. For consistency with velocity measurements, surface pressure data were converted into a nondimensional pressure coefficient referenced to the freestream dynamic pressure at the model eave height:

$$C_p = (P_m - P_s)/(0.5\ \rho\ V_e^2) \tag{4}$$

where

C_p = mean surface pressure coefficient
P_m = mean pressure at model surface (Pa)
P_s = mean static reference pressure (Pa)

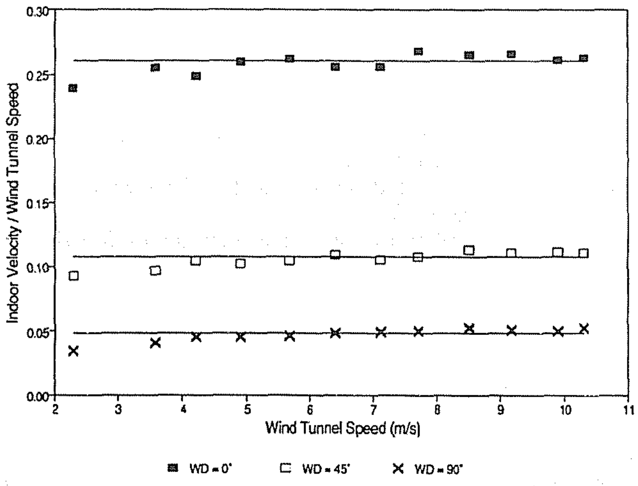

Figure 4 *Reynolds mumber independence test*

ρ = density of air (kg/m^3)
V_e = mean reference velocity at eave height (m/s).

Since the reference freestream velocity at the building's eave height could not be measured simultaneously with the model's surface pressures, the computation of the pressure coefficients was made in two stages. During the tests, the reference freestream velocity used was measured at the pitot tube. This measured value was then corrected to account for the height effect. In this case, the height-correction factor for the reference velocity is the ratio of the velocity at eave height (3.94 in. [100 mm]) to the velocity measured at the pitot tube in the approach flow. This factor was measured in a separate independent test. The estimated error associated with the mean pressure measurements in the dimensionless pressure coefficient form is 0.07.

For each building configuration tested, the surface pressure was measured on the sealed model (no openings) over the area corresponding to the location of the base case inlet and outlet on the open model (a total of nine pressure taps per opening area). The nine pressure tap readings were then averaged together to produce the pressure coefficient for the opening area. $C_{p,i}$ is the average pressure coefficient for the inlet (defined as the "upwind" window) and $C_{p,o}$ corresponds to the outlet (the "downwind" window). The pressure distribution was measured over the rest of the model's surface for only a limited number of configurations.

Correlation Development

The experimental results were analyzed using a PC-based data analysis program. Correlations were developed using a stepwise multiple linear regression fitting routine. In all cases, the terms of the correlation equations are significant beyond 10^{-4}. Full details of the experimental methods are described in Ernest et al. (1990).

RESULTS AND DISCUSSION

Prior to performing the detailed parametric tests in the wind tunnel, a series of preliminary experiments were carried out to investigate the effects of Reynolds number independence and boundary layer roughness. Pressure distributions on the base case model were also compared with currently available published data.

Reynolds Number Independence Tests

One of the similarity criteria for wind tunnel studies of natural ventilation at model scale is the Reynolds number. In theory, the Reynolds number for the flow in the small-scale model should be equal to that obtained for the full-scale building. In practice, however, matching the Reynolds number would be virtually impossible since it would require a wind tunnel speed 30 times higher than that of the natural wind. Fortunately, studies on this problem have indicated that this requirement can be relaxed provided the Reynolds number is higher than a minimum value (Cermak et al. 1982). In the case of interior airflows, it was found that Reynolds number independence was achieved when

$$Re_i = V_w H/\nu > 2 \times 10^4 \tag{5}$$

where

Re_i = interior Reynolds number
V_w = velocity at the inlet window (m/s)
H = height of the model (m)
ν = kinematic viscosity of air (m^2/s).

In this study, Reynolds number independence tests for the interior flows were carried out for the cross-ventilated Model 1 with the base case window size (16.7% porosity). Indoor velocities and turbulence were measured with the row of four probes for wind tunnel speeds varying from 400 fpm (2 m/s) to 2,170 fpm (11 m/s) (corresponding to Re_i ranging from 5.5 x 10^3 to 3 x 10^4). Figure 4 shows that the average indoor velocity coefficient computed for the four probes in the central row becomes practically Reynolds number independent regardless of the wind direction for wind tunnel speeds above 790 fpm (4 m/s). This was also true for indoor velocities measured in the recirculating flows in the rest of the space.

For indoor turbulence intensities, it was found that only the jet flow downwind to the inlet was clearly Reynolds number independent at low wind tunnel speeds. In the rest of the space, the turbulence intensities tend to decrease with increasing wind tunnel speeds. However, indoor turbulence intensities stabilize above a wind tunnel speed of about 1,380 fpm (7 m/s). In agreement with Equation 5, this corresponded to a minimum Re_i of approximately 2 x 10^4 for Reynolds number independence. All subsequent tests in the wind tunnel were conducted with a reference speed of 1,560 fpm (7.9 m/s) at the pitot tube. A close monitoring of the wind tunnel speed indicated that its variations over any given test were less than 1%.

Effects of Boundary Layer Roughness

To perform reliable studies of natural ventilation in buildings, the building-wind interactions must be accurately reproduced at model scale. The key wind features to be modeled in the atmospheric boundary layer are the vertical distributions of mean wind speed and turbulence intensity, which are largely determined by surface characteristics upwind of a particular building site.

The variation of wind velocity with height in the lower levels of the atmospheric boundary layer (the region of greatest interest in building-related wind studies) can be represented by the logarithmic velocity profile for a thermally neutral atmosphere (Cook 1978):

$$V(z) = (u_*/k)\ln[(z-d)/z_0] \tag{6}$$

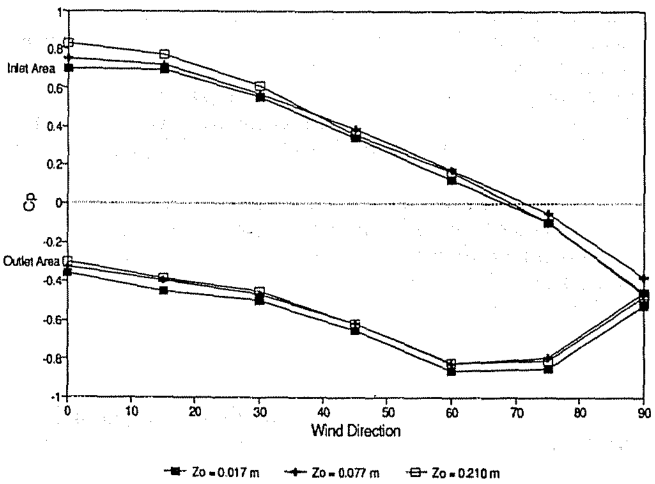

Figure 5a *Effect of boundary layer roughness on mean pressure distributions*

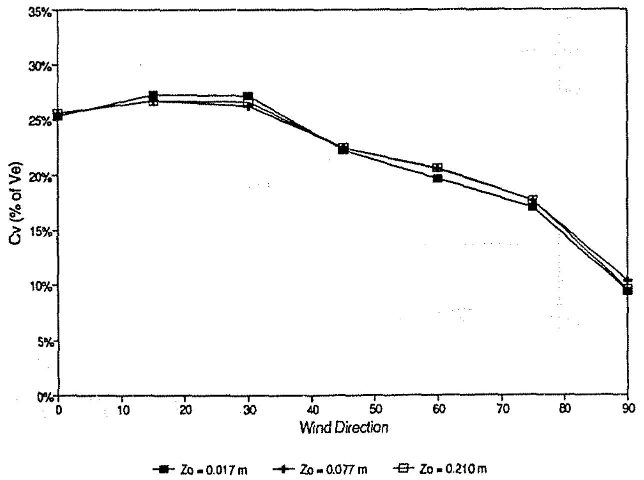

Figure 5b *Effect of boundary layer roughness on interior velocity distributions*

where

$V(z)$ = mean velocity at height z (m/s)
u_* = friction velocity (m/s)
k = von Karman's constant (0.4)
z = height above ground level (m)
d = zero plane displacement height (m)
z_0 = roughness length (m).

The roughness length (z_0) in Equation 6 is a parameter representative of the upwind terrain surface characteristics.

Turbulence intensity is a measure of the magnitude of velocity fluctuations compared with the mean velocity at a point in turbulent flow. Turbulence intensities are always greatest near the ground, where the boundary layer flow interacts with the surface roughness and obstructions, and decreases with increasing height above the ground.

The effect of the boundary layer flow characteristics on the flow pattern inside buildings has not been studied so far; however, it has been previously shown that it can have an effect on the pressure distribution around buildings (Akins and Cermak 1976). For this study, three different types of terrain roughness were modeled to investigate this effect on the base case model (without modeled surroundings). The approaching boundary layer flows were simulated in the wind tunnel using roughness blocks and other flow-processing devices based on techniques described by Cook (1982).

The three terrain roughnesses simulated corresponded to full-scale values of the roughness length (z_0) in Equation 6 of 0.67 in. (0.017 m) (flat farmland), 3.0 in. (0.077 m) (villages), and 8.3 in. (0.210 m) (suburban) (ESDU 1982, 1985).

It was found that when the pressure and velocity data were normalized by the reference velocity at the model's eave height, as in Equations 1 and 4, the change of roughness had virtually no effect. Figure 5a shows the variation of the pressure distribution on the inlet and outlet areas with wind direction for the three roughnesses tested. The small variations are virtually insignificant when compared with variation induced by changes in building geometry. Figure 5b shows the average indoor velocity for the same three profiles. Here again, the effect of roughness change is negligible. The turbulence level of the approaching flow at the model location varied from 16% for the smoothest terrain to 24% for the roughest. This did not significantly affect the turbulence level inside the model, which seems to be generated by the separation at the window edges rather than by external flow conditions. For the rest of the study the roughness length was kept at z_0 = 3.0 in. (0.077 m), corresponding to a relatively smooth terrain typical of villages or the outskirts of small towns.

The measured boundary layer profiles for this roughness length are presented in Figures 6a and 6b. In Figure 6a

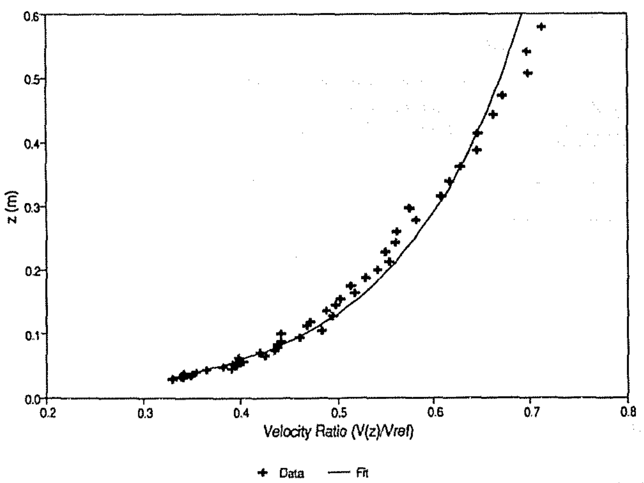

Figure 6a *Mean velocity profile*

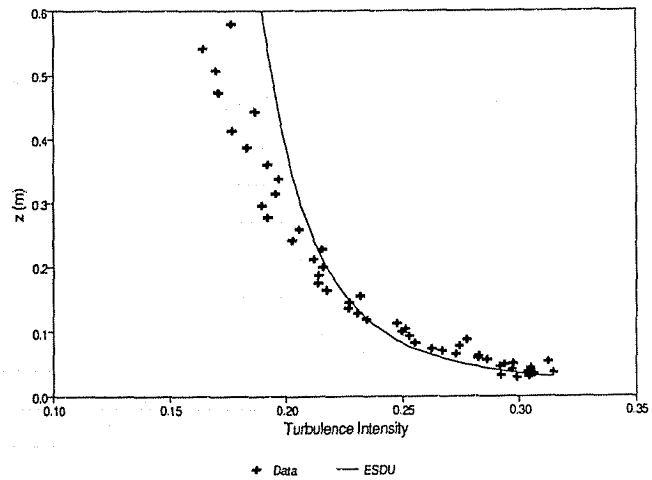

Figure 6b *Turbulence intensity profile*

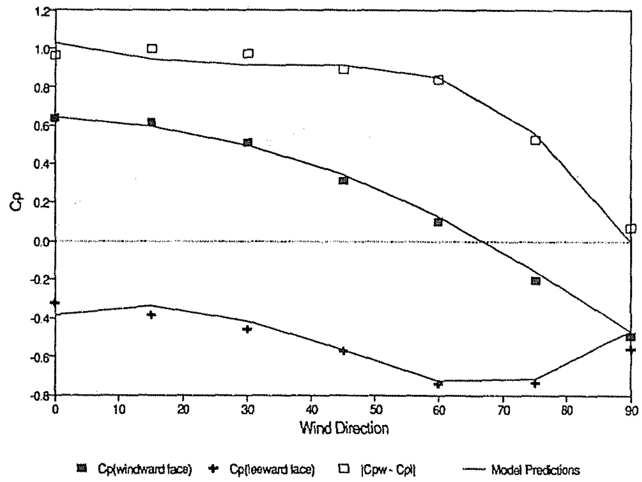

Figure 7 *Comparison of measured data with predictions from Swami and Chandra (1988)*

the solid line represents the regression fit (R^2 = 0.985) of the measured velocities to Equation 6 that produced the roughness length (z_0) of 0.10 in. (2.56 mm) (full-scale z_0 = 3.0 in. [0.077 m]) and a zero plane displacement height (d) of 0 m. In Figure 6b the measured turbulence intensities are compared with recommended values computed for this roughness (represented by the solid line). The comparison shows that measured turbulence intensities for equivalent full-scale heights (z) between 3.3 ft (1 m) and 65.6 ft (20 m) ($\approx$ 1.2 in. [30 mm] and 24 in. [600 mm] at model scale) correspond relatively well to values for this region of the atmospheric boundary layer (ESDU 1984, 1985).

Pressure Distributions on Base Case Model

The surface-averaged pressure distributions measured over the entire wall area of the base case building model were compared with values predicted by Swami and Chandra's model (1988). The model predicts the variation of the wall area surface-averaged pressure coefficient (C_p, referenced to the freestream velocity at the building's eave height) as a function of wind direction and the side aspect ratio (long/short wall length). This model does not directly predict the C_p at normal incidence; instead a reference table provides typical values for that parameter, which are then used as input in the model. Here, the measured value for the surface-averaged pressure coefficient at normal incidence was used as input for the model. This measured pressure coefficient (0.64) is well within the range of previously published values for that parameter. Figure 7 represents the data collected compared with the values predicted by Swami and Chandra's model (solid line) for the wind direction tested. It appears that the agreement is fairly good. However, this experiment also revealed the importance of using local surface pressure data rather than wall-averaged data for the assessment of pressures at inlets and outlets. A description of the full set of parametric tests performed follows.

Effect of Window Size

The effect of window size and wind direction on indoor air motion was investigated for the base case cross-ventilated model configuration with inlet and outlet of equal areas. The average indoor air velocity coefficient (C_v) was measured for 10 different window sizes and for 7 wind directions (every 15° between 0° and 90°). The porosity of the wall was varied from 6% to 25%. The window sizes tested are described in Table 1 and shown in Figure 3a.

The analysis of the variation of the average indoor velocity coefficient to changes in wind angle and wall porosity level revealed that indoor velocity increases with wall porosity at a similar rate regardless of the wind direction. In other words, wind angle (Θ) and porosity (φ) effects are almost independent. Based on this finding, a simple correlation was developed from the 70 data points collected. It was found that the indoor air velocity coefficient could be predicted as a function of the wall porosity and the indoor velocity coefficient obtained for the base case window size (R^2 = 0.984):

$$C_v(\theta,\varphi) = C_v(\theta,\varphi_{bc})\cdot(A\ \varphi + B) \tag{7}$$

where

C_v = average velocity coefficient
Θ = wind direction (0° $\leq \Theta \leq$ 90°)
φ = wall porosity (6% $\leq \varphi \leq$ 25%)
φ_{bc} = base case wall porosity (φ_{bc} = 16.7%).

The coefficients for this equation are

A = 3.52
B = 0.40.

TABLE 1
Window Size Characteristics

Window Number	Width (mm)	Porosity of Wall (φ) % of total wall area	Window/Floor Area Ratio % of total floor area
1	30	6.0%	4.8%
2	40	8.0%	6.4%
3	50	10.0%	8.0%
4	60	12.0%	9.6%
5	70	14.0%	11.2%
6	83.3	16.7%	13.3%
7	90	18.0%	14.4%
8	100	20.0%	16.0%
9	110	22.0%	17.6%
10	125	25.0%	20.0%

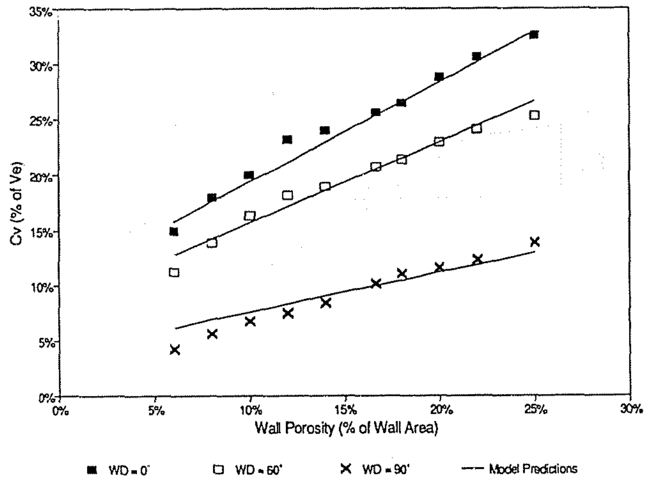

Figure 8 *Effect of window size on indoor velocity distributions*

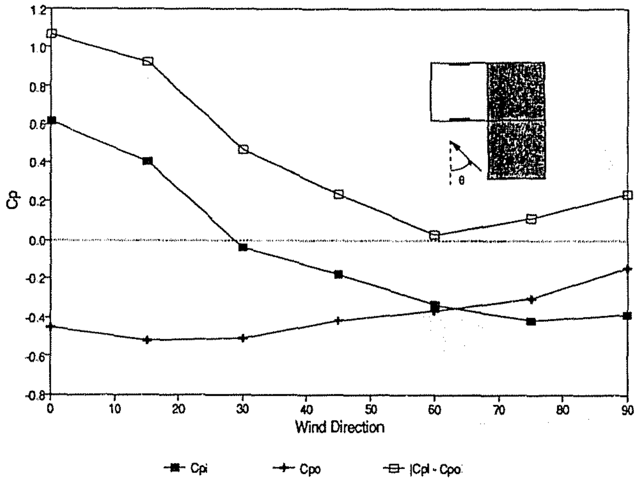

Figure 9a *Mean pressure distributions on L-shaped building*

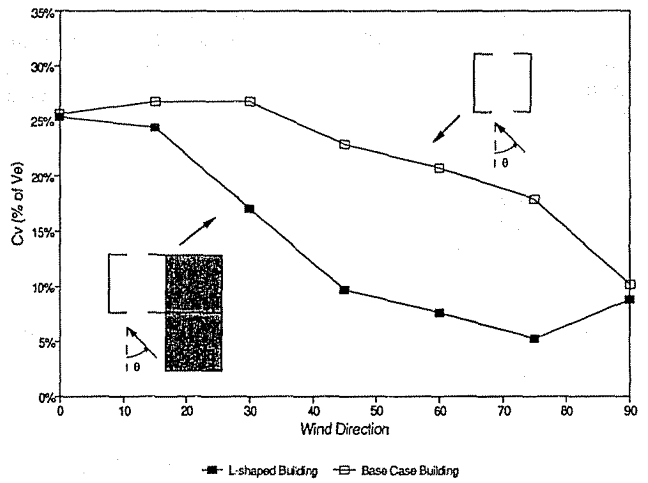

Figure 9b *Indoor velocity distributions in L-shaped building*

This formula, which obviously does not apply to porosities approaching zero, accounts for the fact that C_v increases linearly with φ. Figure 8 shows the measured data compared with correlation Equation 7 for 3 wind angles and for the 10 porosity levels tested.

Effect of External Pressure Distributions

Surface pressure distributions were measured for a total of 32 building configurations that were selected to cover a wide range of possible building-airflow interactions, including the effect of building geometry, upwind obstructions, and other architectural features such as wing walls and roof overhangs. The corresponding indoor air motion parameters were measured for the same configurations and with the base case window size. Each building configuration was tested for the same seven wind directions previously described. The results were then combined into a data base containing a total of 224 sets of pressure and velocity tests.

Figures 9a and 9b present typical examples of such tests. In Figure 9a, the variation of the average pressure distributions over the inlet ($C_{p,i}$) and outlet ($C_{p,o}$) areas of one wing of an L-shaped building with wind direction is presented (see sketch on figure for building configuration). $| C_{p,i} - C_{p,o} |$ represents the available pressure difference across the sealed model. Similarly, the variation of the average velocity coefficient (C_v) for the open L-shaped model, compared with that of the base case model, is shown in Figure 9b. It can be seen from these figures that the pressure field around the building is significantly affected by its geometry (the pressure distribution on the base case model configuration is shown in Figure 5a). As one might expect, the indoor velocity distribution is also affected.

It was generally found that the effectiveness of the pressure difference to induce indoor air motion was reduced when the approaching flow had to change its direction before entering the model. This phenomenon normally occurs for oblique wind angles ($\Theta \geq 45°$) but also when wing walls are present. Moreover, it was found that the strength of the suction zone was more effective at inducing the airflow through the model than the corresponding force of the positive pressure front on the windward side. This finding, similar to that of Gandemer and Barnaud (1989), could have major architectural implications in the design of naturally ventilated buildings. Detailed analysis and presentation of the indoor velocity and surface pressure results are reported in Ernest et al. (1990).

The 224 pressure and velocity data sets collected were used to produce correlations relating the surface pressure and wind direction data to the measured indoor velocities. First, it was of interest to assess to what extent indoor velocity can be related to the available pressure difference measured across the sealed model. Presumably, this pressure difference is the primary driving force for the interior flow. A correlation, independent of wind direction and based on the following equation, was therefore produced:

$$C_v(\Delta C_p) = A\ (\Delta C_p)^{1/2} \tag{8}$$

where

C_v = average velocity coefficient
ΔC_p = $| C_{p,i} - C_{p,o} |$.

The coefficient for this equation is

A = 0.2214.

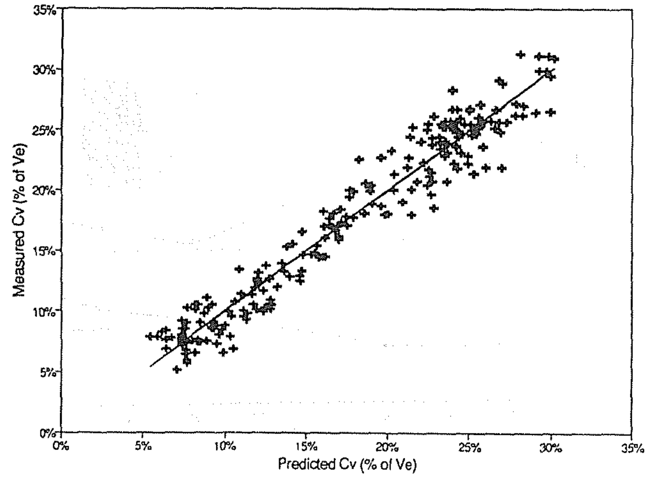

Figure 10a Correlation fit

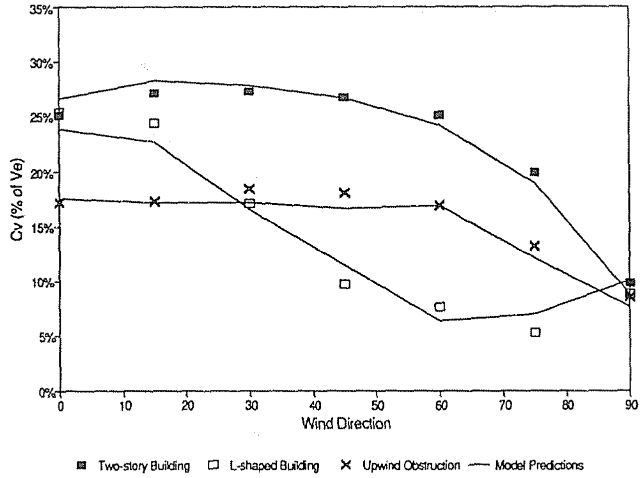

Figure 10b Measurements vs. predictions

Given the probable causal link between $(\Delta C_p)^{1/2}$ and C_v, it was found that the correlation coefficient for this function was relatively low ($R^2 = 0.856$). This could be attributed to the fact that several factors identified during the tests are not accounted for in the equation:

1. The negative suction pressure is more effective than the positive pressure front.
2. The effective area of the opening is reduced with wind angle.
3. A "momentum flow" component is present for small wind angles at the inlet.
4. A residual turbulence-induced flow occurs when $\Delta C_p = 0$.
5. The discharge coefficient for the window may vary with wind angle.

Based on these factors, more complex correlations were developed. To better account for the particular effect of inlet and outlet pressures, the square of the average indoor velocity coefficient (C_v^2) was used as the dependent variable in the correlation. In this case, a correlation ($R^2 = 0.946$ for the predicted values of C_v) was developed to produce the following equation:

$$C_v^2(\theta, C_{p,i}, C_{p,o}) = A\,\Delta C_p + B\,C_{p,i}\cos\theta + C\,C_{p,o}\cos\theta + D\cos\theta + E \qquad (9)$$

where

C_v = average velocity coefficient
θ = wind direction ($0° \leq \theta \leq 90°$)
$C_{p,i}$ = average pressure coefficient for the upwind opening area
$C_{p,o}$ = average pressure coefficient for the downwind opening area
ΔC_p = $|C_{p,i} - C_{p,o}|$.

The coefficients for this equation are:

A = 0.0203
B = 0.0296
C = -0.0651
D = -0.0178
E = 0.0054.

It must be noted that while A, B, and C are independent of the reference velocity used, the coefficients D and E need to be multiplied by the correction factor $(V_e/V_r)^2$ if V_r is used as the reference velocity for the pressure coefficient data instead of V_e.

Equation 9 accounts for some of the factors mentioned above. First, the weight of the pressure coefficient for the outlet is more important than that of the inlet regardless of the wind direction. Second, the effectiveness of wind pressures is reduced with increasing wind angle. Finally, a nonzero indoor velocity level is obtained for $\Delta C_p = 0$ to account for the effect of turbulence-induced ventilation. In the absence of mean wind-pressure driving forces, indoor velocity resulting from wind turbulence remains at its minimum level of about 7% of V_e, a level comparable to that obtained for single-sided ventilation designs. The correlation fit for Equation 9 is presented in Figure 10a. Figure 10b shows the predictions of the model compared with the measured data for three building configurations.

For the average indoor turbulence level, the analysis of the data for the 224 tests revealed that the coefficient of turbulence, C_t, could be approximated by a constant ($R^2 = 0.790$):

$$C_t = 0.538. \qquad (10)$$

The fairly high value of this coefficient, which has the form of a turbulence intensity, indicates that the interior flows are, on the average, very turbulent.

A control test was undertaken to assess the applicability of the prediction (Equation 9) to configurations not used to generate the model. The control test configuration was a complex but repeatable landscaped configuration that included blocks, trees, and other architectural features that had not been previously tested. Here again, the pressure and indoor velocity were measured. The measured surface pressure coefficients (Figure 11a) were used to predict the indoor velocity coefficients in the building. Figure 11b shows the comparisons between the values predicted by Equation 9 and the actual measured velocity coefficients. The largest absolute discrepancy occurs at $\theta = 60°$, where the model underestimates the average indoor velocity by 4% (measured $C_v = 29\%$ vs. predicted $C_v = 25\%$). Overall, the predictions of the model are within the margin of error for the velocity coefficients.

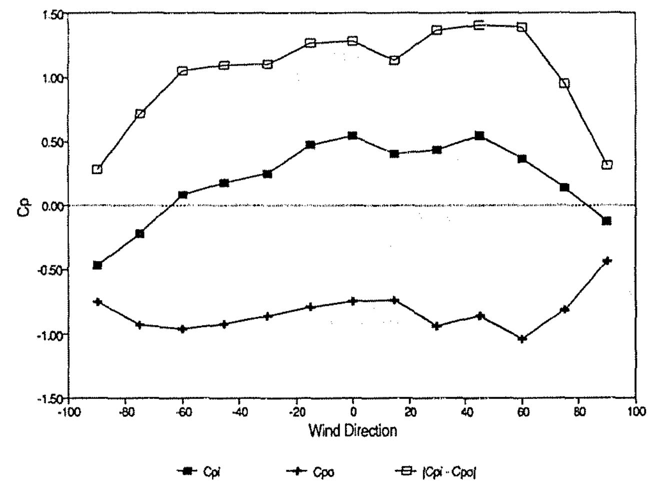

Figure 11a Mean pressure distributions on the control test configuration

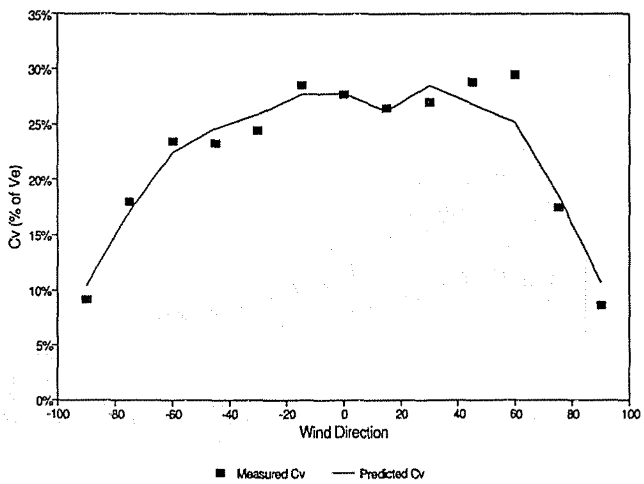

Figure 11b Measurements vs. predictions for the control test configuration

Prediction of Spatial Indoor Velocity Distributions

Local interior velocities can greatly differ from the average indoor velocity depending on the location within the space. In most cases, the velocity will be highest in the jet flow downwind of the inlet and lowest in the node of some recirculating eddy in the room. The overall spread of the local indoor velocity distributions is given by C_{sv}, as defined in Equation 2. The jet flow, which occupies a relatively limited part of the space, dissipates into the rest of the room by distributing its kinetic energy. To analyze the formal structure of this flow distribution, each local measured indoor velocity ratio was expressed as a function of C_{sv}, C_v, and a nondimensional, reduced velocity $\underline{V}$ as follows:

$$V_i/V_e = (\underline{V}_i \cdot C_{sv} + 1) \cdot C_v \qquad (11)$$

where

V_i = mean velocity at interior location i (m/s)
V_e = mean outdoor reference freestream velocity at eave height (m/s)
$\underline{V}_i$ = reduced mean velocity at interior location i
C_{sv} = coefficient of spatial variation
C_v = average velocity coefficient.

In this expression, $\underline{V}_i$ is negative for a local V_i/V_e less than C_v and positive when V_i/V_e is greater than C_v ($\underline{V}_i = 0$ when $V_i/V_e = C_v$). Using this reduced velocity, the overall form of the spatial distributions of the interior velocities becomes independent of the actual values obtained for C_v and C_{sv}. For the prediction of the distribution of ventilative comfort within the space, one would need to be able to estimate the velocity that is exceeded for a certain percentage of the interior floor area. For this purpose, measured interior reduced velocities were sorted from the highest to the lowest value, and an empirical function was developed to approximate their distribution. It was found that the function relating the reduced velocity to the percentage of the floor area could be well approximated by a logarithmic law:

$$\underline{V}(p) = A \ln(p) + B \qquad (12)$$

where

$\underline{V}(p)$ = reduced mean velocity exceeded for p percent of the floor area
p = percentage of the floor area ($0.05 \leq p \leq 1$).

The coefficients for this equation are

A = -1.262
B = -1.109.

Using this function, the predicted value of $\underline{V}$ for p = 50% is -0.23, which, when substituted in Equation 11, shows that the velocity exceeded for 50% of the space is slightly lower than the mean velocity computed for the entire room.

The coefficient of spatial variation, C_{sv}, that was computed for each test increases with unevenness of the velocity distribution in the space. It was found that this coefficient varies considerably depending on the flow conditions. The lowest values (about 0.2) were obtained when the building model was in the wake of an upwind obstruction, while the highest values (about 0.7) were reached for exposed buildings and with a 60° wind angle. However, formal prediction of C_{sv} was made difficult due to the fact that it cannot be directly related to the surface pressure distributions. Nevertheless, it was also found that C_{sv} did not greatly affect the distributions predicted by Equations 11 and 12, if approximated by a constant average value:

$$C_{sv} = 0.495. \qquad (13)$$

Using this value, the predicted velocity distributions in the L-shaped model for three wind directions were compared with the measured local indoor velocities. Figure 12 shows the indoor velocities that are exceeded over a certain percentage of the floor area. The data points for each wind direction correspond to the 20 measured local indoor velocities sorted from the highest to the lowest. Each interior measurement location covers 5% of the floor area of the model. The solid line represents the predicted values for each (V_i/V_e) as derived from Equations 11 and 12. The variation of velocities across the interior space can then be used in determining the distribution of ventilative comfort potential within the interior.

CONCLUSIONS

Wind tunnel measurements of surface pressure and indoor velocity distributions have been made for a large set of building configurations. Simplified correlations have been

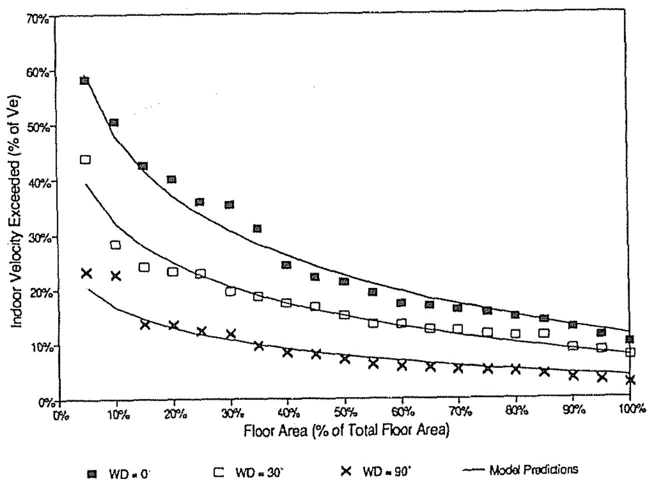

Figure 12 *Prediction of spatial indoor velocity distributions*

developed that allow the prediction of indoor air motion in cross-ventilated buildings as a function of wind direction, window size, and the pressure distribution measured on sealed models with a good level of accuracy. The correlations also permit the prediction of the spatial distribution of the local indoor velocities within the room.

Ongoing research in this project is looking at the effect of simplified interior partitions and window locations. Human comfort and energy implications of this research also will be investigated. Architectural guidelines for the design of naturally ventilated buildings will be suggested.

Future work on indoor air motion is needed to address the following issues:

1. Natural ventilation in multi-room buildings.
2. Effect of interior room geometry (ceiling height, width/length ratio, furniture, and partitions).
3. Effect of window accessories (louvers, screens).
4. Effect of turbulence intensity on human comfort in naturally ventilated environments.

ACKNOWLEDGMENTS

The work described in this study was funded by a grant from the Universitywide Energy Research Group at the University of California. The authors wish to acknowledge Alison Kwok of the UC-Berkeley Architecture Department for her help with the model construction and figures.

NOMENCLATURE

C_d = discharge coefficient, nondimensional
C_p = pressure coefficient (Equation 4), nondimensional
$C_{p,i}$ = average pressure coefficient for the upwind opening area, nondimensional
$C_{p,o}$ = average pressure coefficient for the downwind opening area, nondimensional
C_{sv} = coefficient of spatial variation (Equation 2), nondimensional
C_t = average turbulence coefficient (Equation 3), nondimensional
C_v = average velocity coefficient (Equation 1), nondimensional
d = zero plane displacement height, m
H = height of models, m
k = von Karman's constant (0.4), nondimensional
n = number of interior velocity measurement locations (20), nondimensional
P_m = mean pressure at model surface, Pa
P_s = mean static reference pressure, Pa
Re_i = interior Reynolds number (Equation 5), nondimensional
u_* = friction velocity, m/s
$\underline{V}$ = reduced mean velocity (Equations 11 and 12), nondimensional
$V(z)$ = mean velocity at height z, m/s
V_e = mean reference velocity at eave height, m/s
V_i = mean velocity at interior location i, m/s
V_w = mean velocity at the inlet window, m/s
z = height above ground level, m
z_0 = roughness length, m

Greek Letters

φ = wall porosity (window area/wall area), nondimensional
ν = kinematic viscosity of air, m²/s
θ = wind direction with respect to outward normal of windward wall, degrees
ρ = density of air, kg/m³
σ_s = standard deviation over space
σ_t = standard deviation over time
Δ = absolute value of difference
Σ = summation

REFERENCES

Akins, R.E., and J.E. Cermak. 1976. "Wind pressures on buildings." Fluid Dynamics and Diffusion Laboratory, Report CER76-77REA-JEC15. Fort Collins: Colorado State University.

Arens, E.A., and N.S. Watanabe. 1986. "A method for designing naturally cooled buildings using bin climate data." *ASHRAE Transactions*, Vol. 92, Part 2B.

Arens, E.A., A.G. Blyholder, and G.E. Schiller. 1984. "Predicting thermal comfort of people in naturally ventilated buildings." *ASHRAE Transactions*, Vol. 90, Part 1B.

Arens, E.A., R. Gonzalez, and L. Berglund. 1986. "Thermal comfort under an extended range of environmental conditions." *ASHRAE Transactions*, Vol. 92, Part 1.

Arens, E.A., D. Ballanti, C.Bennett, S. Guldman, and B. White. 1989. "Developing the San Francisco wind ordinance and its guidelines for compliance." *Building and Environment*, Vol. 24, No. 4, pp. 297-303.

Aynsley, R.M. 1982. "Natural ventilation model studies." *Proceedings of the International Workshop on Wind Tunnel Modeling Criteria and Techniques for Civil Engineering Applications*, pp. 465-485. Cambridge, NY: Cambridge University Press.

Aynsley, R.M. 1988. "A resistance approach to estimating airflow through buildings with large openings due to wind." *ASHRAE Transactions*, Vol. 94, Part 2.

Balazs, K. 1989. "A wind pressure database from Hungary for ventilation and infiltration calculations." *Air Infiltration Review*, Vol. 10, No. 4.

Bauman, F.S., D.R. Ernest, and E.A. Arens. 1988. "The effects of surrounding buildings on wind pressure distributions and natural ventilation in long building rows." *ASHRAE Transactions*, Vol. 94, Part 2, pp. 1670-1695.

Cermak, J.E., M. Poreh, J.A. Peterka, and S.S. Ayad. 1982. "Wind tunnel investigations of natural ventilation." American Society of Civil Engineers Convention and Exhibit Preprint 82-519, New Orleans, LA.

Chand, I. 1968. "Effect of height of sill on indoor air motion." *Journal of the Institution of Engineers (India) CI*, Vol. 49, pp. 136-139.

Chand, I. 1970. "Effect of the distribution of fenestration area on the quantum of natural ventilation in buildings." *Architectural Science Review*, Vol. 13, No. 2, pp. 130-133.

Chand, I., and N.L.V. Krishak. 1969. "Effect of window size, location and orientation on indoor air motion." *Journal of the Institution of Engineers (India) CI*, Vol. 49, pp. 375-378.

Chand, I., N.L.V. Krishak, and V.K. Sharma. 1975. "Studies of air motion in shielded buildings." *The Indian Architect*, Vol. 19, No. 9, pp. 23-29.

Chand, I., V.K. Sharma, and P.K. Bhargava. 1978. "Effect of height and type of roof on air motion in industrial buildings." *The Indian Architect*, pp. 115-119.

Chand, I., V.K. Sharma, and N.L.V. Krishak. 1989. "Ventilation survey of typical airy buildings—A few case studies in hot dry and hot humid zones of India." *Building and Environment*, Vol. 24, No. 3, pp. 229-238.

Chandra, S., A. Kerestecioglu, P. Fairey, and W. Cromer. 1982. "Comparison of model and full-scale natural ventilation studies." *Proceedings of the International Workshop on Wind Tunnel Modeling Criteria and Techniques for Civil Engineering Applications*, pp. 669-684. Cambridge, NY: Cambridge University Press.

Chang, S.K.W., E.A. Arens, and R.R. Gonzalez. 1988. "Determination of the effect of walking on the forced convection heat transfer coefficient using an articulated mannikin." *ASHRAE Transactions*, Vol. 94, Part 1.

Cook, N. 1978. "Wind tunnel simulation of the adiabatic atmospheric boundary layer by roughness, barrier and mixing-device methods." *Journal of Industrial Aerodynamics*, Vol. 3, pp. 157-176.

Cook, N. 1982. "Simulation techniques for short test-section wind tunnels: roughness, barrier and mixing-device methods." *Proceedings of the International Workshop on Wind Tunnel Modeling Criteria and Techniques for Civil Engineering Applications*, pp. 126-136. Cambridge, NY: Cambridge University Press.

Coutier, J.P., R.C. Kammerud, and J.W. Place. 1985. "Thermal comfort of building occupants: A preliminary impact assessment of passive strategies." *ASHRAE Transactions*, Vol. 91, Part 2A, pp. 62-74.

Ernest, D.R., F.S. Bauman, and E.A. Arens. 1990. *The prediction of indoor air motion for occupant cooling in naturally ventilated buildings*. Berkeley: Center for Environmental Design Research, University of California.

ESDU. 1982. *Strong winds in the atmospheric boundary layer*. Item No. 82026. London: Engineering Sciences Data Unit International Ltd.

ESDU. 1984. *Longitudinal turbulence intensities over terrain with roughness changes for flat or hilly sites*. Item No. 84030. London: Engineering Sciences Data Unit International Ltd.

ESDU. 1985. *Characteristics of atmospheric turbulence near the ground*. Item No. 85020. London: Engineering Sciences Data Unit International Ltd.

Fanger, P.O., A. Melikov, and H. Hanzawa. 1988. "Air turbulence and sensation of draft." *Energy and Buildings*, Vol. 12, No. 1.

Gandemer, J., and G. Barnaud. 1989. "Ventilation naturelle en climat tropical humide: Prise en compte du vent dans l'habitat." *Proceedings of the 11th Triennial Congress of the Information Council for Building Research, Studies and Documentation (CIB)*, Paris, June, pp. 227-236.

Givoni, B. 1962. "Basic studies of ventilation problems in housing in hot countries." Report of the Building Research Station, Technion, Israel.

Givoni, B. 1965. "Laboratory study of the effect of window size and location on indoor air motion." *Architectural Science Review*, Vol. 8, No. 2, pp. 42-45.

Givoni, B. 1969. *Man, climate and architecture*, 2d ed., pp. 230-277. Amsterdam: Elsevier Publishing Co. Ltd.

Holmes, M.J., and G.E. Whittle. 1987. "How accurate are the predictions of complex air movement models?" *Building Services Engineering Research and Technology*, Vol. 8, No. 2, pp. 29-31.

Jones, B.W., K. Hsieh, and M. Hashinaga. 1986. "The effect of air velocity on thermal comfort at moderate activity levels." *ASHRAE Transactions*, Vol. 92, Part 2.

Kurabuchi, K., and T. Kusuda. 1987. "Numerical prediction for indoor air movement." *ASHRAE Journal*, December, pp. 26-30.

Mathews, E.H., ed. 1989. "Numerical solutions of fluid problems related to buildings, structures and the environment." *Building and Environment*, Vol. 24, No. 1 (special issue).

Mayer, E. 1987. "Physical causes for draft: Some new findings." *ASHRAE Transactions*, Vol. 93, Part 1.

McIntyre, D.A. 1978. "Preferred air speeds for comfort in warm conditions." *ASHRAE Transactions*, Vol. 84, Part 1, pp. 264-277.

Pedersen, C.O., J.D. Spitler, C.E. Fisher, P.F. Menne, and J. Cantillo. 1990. *Standard hourly energy calculation methods for predicting performance of ventilative cooling*. Final Report, ASHRAE 529-RP. Department of Mechanical and Industrial Engineering, University of Illinois at Urbana-Champaign.

Poreh, M., J.E. Cermak, and J.A. Peterka. 1982. "Wind tunnel research of flowfields within naturally ventilated rooms of simple geometry." Fluid Dynamics and Diffusion Laboratory, Report CER82-83MP-JEC-JAP17. Fort Collins: Colorado State University.

Scheatzle, D.G., H. Wu, and J. Yellott. 1989. "Extending the summer comfort envelope with ceiling fans in hot, arid climates." *ASHRAE Transactions*, Vol. 95, Part 1, pp. 269-280.

Snyckers, W.A. 1970. "Wind tunnel studies of the flow of air through rectangular openings with application to natural ventilation of buildings." M.S. thesis, University of Pretoria, South Africa.

Sobin, H. 1981. "Window design for passive ventilative cooling: An experimental model-scale study." *Proceedings of the 1981 International Passive/Hybrid Cooling Conference*, pp. 191-195.

Sobin, H. 1983. *Analysis of wind tunnel data on naturally ventilated models*. Tucson, AZ: Harris Sobin Assoc.

Swami, M.V., and S. Chandra. 1988. "Correlations for pressure distribution on buildings and calculation of natural-ventilation airflow." *ASHRAE Transactions*, Vol. 94, Part 1, pp. 243-266.

Tanabe, S., and K. Kimura. 1989. "Importance of air movement for thermal comfort under hot and humid conditions." *Proceedings of the ASHRAE Far East Conference on Air-Conditioning in Hot Climates*, Kuala Lumpur, Malaysia, October 25-29.

Tsutsumi, J., T. Katayama, T. Hayashi, Q. Zhang, and H. Yoshimizu. 1988. "Numerical simulation of indoor turbulent air flows caused by cross-ventilation and its model experiments." *Effective Ventilation, 9th AIVC Conference*, Ghent, Belgium, September 12-15, pp. 141-156.

Vickery, B.J., and C. Karakatsanis. 1987. "External wind pressure distributions and induced internal ventilation flow in low-rise industrial and domestic structures." *ASHRAE Transactions*, Vol. 93, Part 2, pp. 2198-2213.

DISCUSSION

J. van der Maas, EPFL-LESO, Lausanne, Switzerland: Your model was not aiming at measuring ventilation, but with what accuracy can you assess ventilation as well?

D.R. Ernest: This model cannot be used to directly predict wind-induced natural ventilation airflow rates. However, it can be used to estimate the maximum indoor velocity measured very close to the inlet opening. This velocity can then be used to assess the airflow rate through that opening. However, no airflow rate measurements were conducted to evaluate the accuracy of this assessment.